Clinical Cancer Research

PIK3CA Mutations Contribute to Acquired Cetuximab Resistance in Patients with Metastatic Colorectal Cancer

Jian-Ming Xu[1], Yan Wang[1], You-Liang Wang[2], Yan Wang[3,4], Tao Liu[5], Ming Ni[6], Man-Sheng Li[7], Li Lin[1], Fei-Jiao Ge[1], Chun Gong[3], Jun-Yan Gu[3], Ru Jia[1], He-Fei Wang[1], Yu-Ling Chen[1], Rong-Rui Liu[1], Chuan-Hua Zhao[1], Zhao-Li Tan[1], Yang Jin[1], Yun-Ping Zhu[7], Shuji Ogino[8,9,10], and Zhi-Rong Qian[10]

Abstract

Purpose: Mutations in *KRAS* are considered to be the main drivers of acquired resistance to epidermal growth factor receptor (EGFR) blockade in patients with metastatic colorectal cancer (mCRC). However, the potential role of other genes downstream of the EGFR signaling pathway in conferring acquired resistance has not been extensively investigated.

Experimental Design: Using circulating tumor DNA (ctDNA) from patients with mCRC and with acquired cetuximab resistance, we developed a targeted amplicon ultra-deep sequencing method to screen for low-abundance somatic mutations in a panel of genes that encode components of the EGFR signaling pathway. Mutations with significantly increased variant frequencies upon disease progression were selected by using quartile analysis. The functional consequences of the identified mutations were validated in cultured cells.

Results: We analyzed 32 patients with acquired cetuximab resistance in a development cohort. Of them, seven (22%) carried five novel *PIK3CA* mutations, whereas eight (25%) carried previously reported *KRAS* mutations. Functional studies showed that novel *PIK3CA* mutations (all in exon 19; p.K944N, p.F930S, p.V955G, p.V955I, and p.K966E) promote cell viability in the presence of cetuximab. Only one novel *PIK3CA* mutation (p.K944N) was verified in one of the 27 patients with acquired resistance in a validation cohort, simultaneous *KRAS* and *PIK3CA* hotspot mutations were detected in two patients. Among the above 59 acquired resistance patients, those with *PIK3CA* or *RAS* mutations detected in ctDNA showed a pronounced decrease in progression-free survival than patients with no mutation.

Conclusions: The *PIK3CA* mutations may potentially contribute to acquired cetuximab resistance in patients with mCRC.
Clin Cancer Res; 23(16); 4602–16. ©2017 AACR.

Introduction

Epidermal growth factor receptor (EGFR) signaling promotes cell proliferation and migration, and the constitutive activation of this pathway is associated with tumor progression and metastasis in colorectal cancer. Anti-EGFR antibodies, such as cetuximab, improve the survival of patients with metastatic colorectal cancer (mCRC). Cetuximab is currently recommended for patients with mCRC expressing wild-type *RAS* (1). However, in a large proportion of patients who respond, acquired resistance to cetuximab emerges despite the absence of detectable mutations in *RAS*.

It is now clear that embryologic origin of the colon contributes to the genomic profile of a colorectal cancer and has implications on prognosis and response to specific therapeutics. Right-sided colon cancers have embryologic origin in the midgut and have higher rates of microsatellite instability, gene promoter hypermethylation leading to gene silencing, and BRAF mutation, whereas left-sided tumors originate from the hindgut and have a genomic profile distinct from right-sided tumors. Recently, many studies (2–4) demonstrated that the predictive value of the location was mainly related to the response to biologic agents, cetuximab, and bevacizumab, of which, cell proliferation and developmental pathways, such as RAF/RAS/ERK/MEK and mTOR/PI3K/AKT pathways, could play vital roles in response to anti-EGFR antibody, cetuximab.

Recent studies have implicated mutations in several other genes in the EGFR signaling pathway, such as *BRAF*, *PIK3CA*, and *PTEN*, in the acquisition of resistance to cetuximab (5–7). However, it remains to be determined whether such resistance-causing mutations were present in the primary tumor or occurred during

[1]Affiliated Hospital Cancer Center, Academy of Military Medical Sciences, Beijing, China. [2]Beijing Institute of Biotechnology, Beijing, China. [3]QuestGenomics Biotechnology Co, Ltd. Nanjing, Jiangsu, China. [4]Gnomegen, San Diego, California. [5]Center of Computational Biology, Institute of Basic Medical Sciences, Beijing, China. [6]Beijing Institute of Radiation Medicine, Beijing, China. [7]Beijing Proteome Research Center, Beijing Institute of Radiation Medicine, Beijing, China. [8]Division of MPE Molecular Pathological Epidemiology, Department of Pathology, Brigham and Women's Hospital, and Harvard Medical School, Boston, Massachusetts. [9]Department of Epidemiology, Harvard T.H. Chan School of Public Health, Boston, Massachusetts. [10]Department of Oncologic Pathology, Dana-Farber Cancer Institute, and Harvard Medical School, Boston, Massachusetts.

Note: Supplementary data for this article are available at Clinical Cancer Research Online (http://clincancerres.aacrjournals.org/).

J.-M. Xu, Y. Wang, Y.-L. Wang, and Y. Wang contributed equally to this article.

Corresponding Author: Jian-Ming Xu, Affiliated Hospital Cancer Center, Academy of Military Medical Sciences, No. 8 Dong Avenue, Fengtai District, Beijing 100071, China. Phone: 861051128358; Fax: 861051128358. E-mail: jmxu2003@yahoo.com

doi: 10.1158/1078-0432.CCR-16-2738

Translational Relevance

Acquired resistance to cetuximab limits its application in clinical practice. In addition to *RAS* mutations, other genes downstream of the EGFR signaling pathway might be involved in acquired resistance to cetuximab. We have designed an innovative strategy to identify low-frequency candidate mutations that are associated with acquired cetuximab resistance, by sequencing circulating tumor DNA taken from metastatic colorectal cancer (mCRC) patient plasma samples, obtained before and during treatment. This quartile-based selection strategy helped us to identify mutations that started at extremely low allelic fractions but increased in frequency during treatment, independently of the identification of existing somatic mutations in tumor tissues or in known "hot-spots." We have identified five novel mutations in exon 19 of *PIK3CA*, which contribute to acquired cetuximab resistance. The importance of *PIK3CA* mutations in acquired cetuximab resistance highlights the potential therapeutic benefit of combining a PIK3CA inhibitor with an anti-EGFR antibody in the treatment of mCRC.

treatment. Diaz and colleagues have previously reported that *KRAS* mutations were responsible for acquired resistance to EGFR blockade in nine of 24 patients with mCRC (8). We hypothesized that in addition to *KRAS*, mutations in genes downstream of EGFR may also confer acquired resistance to cetuximab-based therapy.

Recent studies have used next-generation sequencing (NGS) to test for specific mutations in circulating tumor DNA (ctDNA) obtained from patient plasma. However, these studies monitored mutations identified in tumor tissue from the same patient or known "hot-spot" mutations (9–14); hence, any other mutations emerging during treatment that results in acquired resistance are likely to have been missed.

Here, we have evaluated a panel of genes that are thought to play pivotal roles in the activation of the EGFR signaling pathway or frequently mutated in colorectal cancer. We overcome these previous limitations by employing ultra-deep amplicon sequencing technology and a newly developed data analysis approach, and we describe the identification of emergent resistant mutations in ctDNA from longitudinal plasma samples obtained from patients with mCRC based on dynamic changes in allelic fractions. By analyzing structural and functional changes, as well as the clinical influence of these mutations, we extend our existing knowledge of mutations that contribute to acquired cetuximab resistance.

Materials and Methods

Patients and sample collection for the development cohort

We performed a retrospective single-center study at the Affiliated Hospital, Academy of Military Medical Sciences, Beijing, China. Eligible patients (see Supplementary Materials and Methods) had pathologically confirmed mCRC harboring wild-type *KRAS* codons 12 and 13 and wild-type *BRAF* codon 600, as determined via Sanger sequencing of the tumor tissue DNA. *NRAS* was not recommended for routine testing at the onset of the study in 2011 (15). Patients received cetuximab treatment with or without chemotherapy. Prior treatments were permitted except for cetuximab. Serum carcinoembryonic antigen (CEA) and cancer antigen 19-9 (CA 19-9) levels were measured during each therapeutic cycle. Computed tomography (CT) scans were performed and reviewed every 6 to 8 weeks to evaluate clinical response using the Response Evaluation Criteria in Solid Tumors (RECIST), version 1.1 (16). Clinical data including response evaluation during the study were collected. Longitudinal blood samples (4 mL) from each patient were obtained at baseline and every 4 weeks until disease progression or until the last plasma sample was collected. Formalin-fixed paraffin-embedded (FFPE) tumor tissues and peripheral blood mononuclear cells were also collected before treatment. Blood specimens were frozen at −80°C and were linked to demographic, clinical, and genetic data stored in a secure research database. This study protocol was approved by the local ethics committee (KY-2011-8-3), and was conducted in accordance with International Ethical Guidelines for Biomedical Research Involving Human Subjects (CIOMS). Written informed consent was obtained from each patient.

Sample processing and amplicon sequencing

Following DNA extraction and quantification, samples from plasma and tumor tissues were both subjected to amplicon deep sequencing (see Supplementary Materials and Methods) for the following target regions, which are thought to play pivotal roles in the activation of the EGFR signaling pathway or frequently mutated in colorectal cancer: *AKT1* (exon 3), *BRAF* (exon 15), *EGFR* (exons 10 and 12), *KRAS* (exons 2, 3, and 4), *NRAS* (exons 2, 3, and 4), *PIK3CA* (exons 8 and 19), *PTEN* (exons 5, 7, and 8), and *TP53* (exons 5, 6, and 7; refs. 6, 17, 18), as well as the splice site regions of these exons (i.e., intronic regions within 4 bp of an exon/intron boundary).

The amplicon libraries were subjected to deep sequencing using a Proton System (Life Technologies). The primer sequences are provided in Supplementary Materials and Methods. Targeted average sequencing depths were 1,000 × for FFPE tumor tissue or blood cell DNA samples and 10,000 × for cfDNA samples. All testing was conducted by an independent laboratory supplied with blinded samples. (QuestGenomics Biotechnology Co, Ltd.).

Identification of mutations associated with acquired resistance

After routine quality control and data processing steps, we called single-nucleotide variants (SNVs) without filtering for any variant frequencies. Somatic mutations were identified by comparing SNVs from the genomic DNA extracted from peripheral blood mononuclear cells and FFPE samples. Using quartile analysis, mutations with significantly increased variant frequencies upon disease progression, or those that were present only during disease progression, were identified as candidate mutations associated with acquired resistance. Deep-sequencing data processing, SNV calling, and quartile analysis are described in the Supplementary Materials and Methods. Mutations were annotated using SNPnexus (19). All nonsynonymous mutations were further analyzed using PolyPhen-2 and SIFT to determine their potential effects on protein function (20, 21). Variants predicted to be "damaging" by both PolyPhen-2 and SIFT were selected for further analysis. The workflow was shown in Supplementary Fig. S1.

Functional analysis of *PIK3CA* mutations

Structure modeling and functional analysis. MODELLER (version 9v6; ref. 22) was used for homology modeling. Three-

dimensional (3D) structures of wild-type and mutant PIK3CA binding to PIK3R1 were modeled using the 3D structure of 4JPS in the PDB (Protein Data Bank) database as a template (23). Hydrogen atoms were added using CHARMM (version c32b2; ref. 24). The protonation states of titratable residues were determined using an in-house CHARMM script (25). VMD (version 1.9.1; ref. 26) was used to view and analyze the modeled structures.

In vitro functional assays. The *PIK3CA* point mutations identified in ctDNA and FFPE tumor tissue were introduced into the full-length *PIK3CA* coding sequence using site-directed mutagenesis and were inserted into an expression vector (RC213112, Origene). Sequences of the primers used to construct *PIK3CA* mutation expression vectors are provided in Supplementary Materials and Methods. A human colorectal cancer cell line (DiFi) was transfected with the *PIK3CA* mutation expression vectors and assessed by Western blot to identify changes in the phosphorylation levels of AKT and other downstream EGFR targets. The following antibodies were used: Flag (Sigma-Aldrich, Cat. # F3165), p-AKT (Ser473) (Cell Signal, Cat. # 4060), pan-AKT (Cell Signal, Cat. # 4685), p-ERK1/2 (Cell Signal, Cat. # 4367), and total ERK1/2 (Cell Signal, Cat. # 9107). Cell viability analyses were performed to detect sensitivity to cetuximab and/or to 5-fluorouracil (5-FU). The hotspot mutations in *PIK3CA* exons 9 and 20 (p.E542K, p.E545K, and p.H1047R) were included for comparison. Vector construction, Western blot, and cell viability analysis are described in the Supplementary Materials and Methods.

Validation cohort enrollment and sample collection

A validation cohort of patients was prospectively enrolled to verify the acquired resistance mutations detected only in ctDNA after the main data analyses were completed. These patients were enrolled on the same basis as the former patients, the exception being the inclusion of wild-type *NRAS* codons 12 and 13 in the eligibility criteria according to updated studies (1). Longitudinal plasma samples were collected every 4 to 8 weeks during the entire treatment period. Investigators blinded to clinical data conducted mutational analyses independently.

Target gene regions of amplicon sequencing

The following gene regions were added to the former panel for Amplicon deep sequencing: *APC* (exons 14, 15, and 16), *EGFR* (exons 18 to 21), *GNAS* (exons 8), *PIK3CA* (exons 9 and 20), and *TP53* (exons 4b and 8), as well as the splice site regions of these exons. All of these target regions were reported to be frequently mutated in colorectal cancer and are possibly implicated in drug resistance (27, 28). The primer sequences are provided in Supplementary Materials and Methods. The remaining conditions for the next-generation sequencing were the same as for the former experiments.

Statistical analysis

Kaplan–Meier methods were used to estimate progression-free survival (PFS). A univariate Cox regression analysis was performed for each of the variables of interest. The hazard ratio (HR), 95% confidence intervals (CIs), and Wald statistic *P* values are reported for each model. A *P* value of less than 0.05 was considered statistically significant, and an HR greater than 1.5 was considered clinically meaningful due to the small sample size. All statistical tests were performed using SPSS version 20.0 software (IBM).

Results

Patient information

In total, 59 patients from the initial development cohort were screened for eligibility between August 2011 and December 2013. Six patients were excluded from the study due to the lack of suitable tumor samples or of peripheral blood cell samples collected prior to therapy. The remaining 53 patients were enrolled in the study as the development cohort and received at least 4 weeks of cetuximab alone or in combination with chemotherapy. The patients were divided into two groups based on the response evaluation at week 12. We defined primary resistance as PFS < 12 weeks and acquired resistance as PFS $\geq$ 12 weeks (29).

The acquired-resistance group consisted of 20 patients with longitudinal plasma samples (cases 1–20) and 18 patients without longitudinal plasma samples (with only two to three plasma samples including baseline and progression points; cases 21–38). Of the 38 patients with acquired resistance, six patients without longitudinal plasma samples were excluded from further analysis due to the lack of plasma samples at progression. Therefore, a total of 32 patients with acquired resistance were included in the mutational analysis (Fig. 1). As a comparison group, we included 15 primary resistance patients (cases 39–53). Detailed clinical information is provided in Supplementary Table S1.

Investigation of somatic variants in circulating tumor DNA

We sequenced 18 exons from eight genes involved in EGFR signaling, covering approximately 3,000 base pairs. The average sequencing depth (raw data) across all plasma samples reached 9,664 $\times$. We identified more than 20,000 SNVs among all samples processed. The vast majority of the SNVs were present in very low allelic fractions (<0.5%; Fig. 2A). We retained these variants in further analyses, as low-abundance mutations may be functionally relevant.

After screening for the allelic fractions of the SNVs by quartile analysis, we identified an average of 26 SNVs in each patient (Fig. 2B). Only those mutations with allelic fractions significantly higher than the majority were eventually selected as candidate mutations. Overall, we identified 39 nonsynonymous SNVs as candidates across all 32 patients with acquired resistance to cetuximab. Among these 39 nonsynonymous SNVs, 20 mutations were selected as acquired resistance mutations using PolyPhen-2 and SIFT (Supplementary Table S2). Some of these acquired resistance mutations, specifically p.W22G in *AKT1*; p.V600E in *BRAF*; p.K5N, p.G12D, p.G12V, p.G13D, and p.Q61H in *KRAS*; p.M134L and p.Q245* in *PTEN*, are described in the large intestine dataset of the COSMIC database (including in cecum, colon, and rectal cancers), whereas none of the mutations found in *PIK3CA* (p.K944N, p.F930S, p.V955G, p.V955I, and p.K966E) are described in COSMIC (Supplementary Table S2).

Eventually, in the 32 patients with acquired resistance, 14 mutations were present in 10 of the 20 patients with longitudinal plasma samples, and 12 mutations were present in eight of the 12 patients without longitudinal plasma samples. Twenty-five of the 26 mutations exhibited a highly significant difference (*P* value < 0.01) from the background nonreference allelic fractions (Table 1; Supplementary Table S3), whereas none of the candidate mutations were identified in the 15 patients with primary resistance.

The detected acquired mutations were observed most commonly in *PIK3CA* and *KRAS*, with a total of five *PIK3CA* mutations identified in seven of the 32 patients (22%), and five *KRAS*

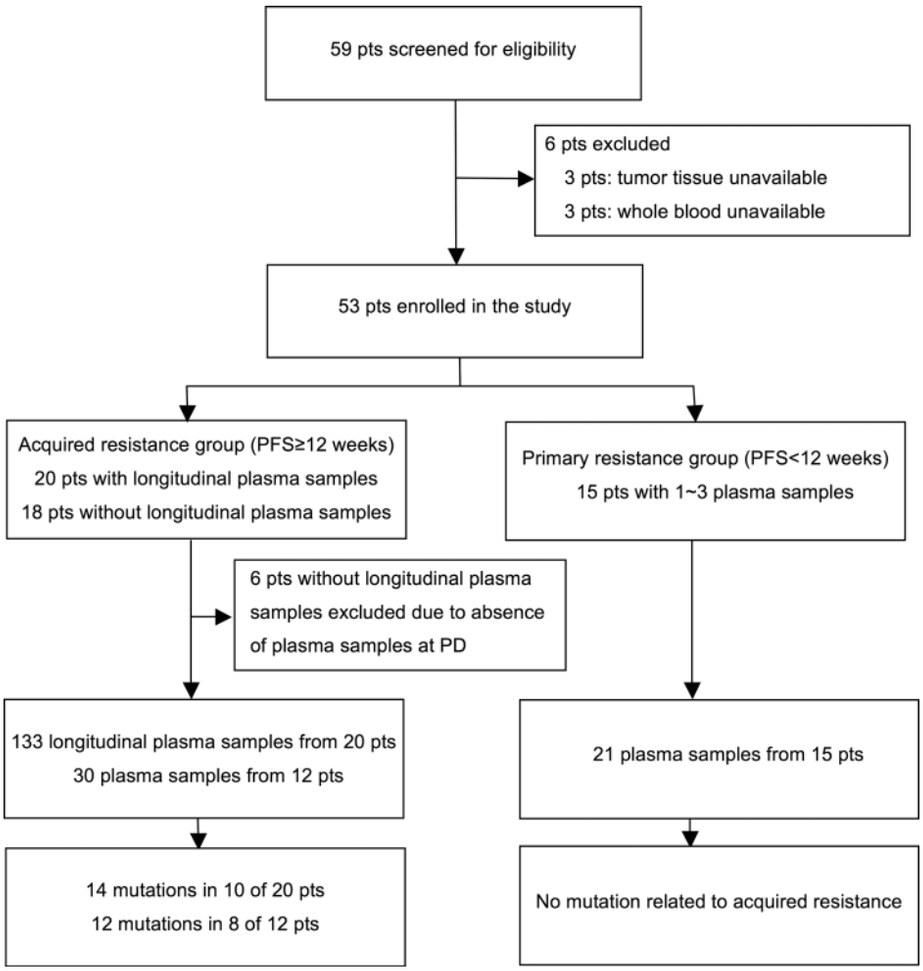

Figure 1.
Workflow of the study. Of the 59 patients screened for eligibility, 53 patients were enrolled in the study and received at least 4 weeks of cetuximab therapy. PD, progressive disease; PFS, progression-free survival; pts, patients.

mutations in eight of the 32 patients (25%; three of these patients harbored a double mutation in *KRAS*). In addition, three point mutations in *BRAF*, including the hotspot mutation c.1799T>A (p.V600E), and sporadic mutations in *AKT1*, *EGFR*, *TP53*, and *PTEN* were identified. Five patients harbored mutations in more than one gene (Fig. 2C).

Analysis of preexisting mutations in tumor tissues

Sixty-two somatic mutations were identified in 30 out of 53 patients. Thirty-nine of these mutations were identified in 22 out of 38 patients with acquired resistance (average two mutations per individual), which mainly clustered in *KRAS* and *TP53* (30.8% each), whereas the remaining 23 mutations were identified in eight out of 15 patients with primary resistance (average three mutations per individual), which were uniformly distributed (17.4% each in *KRAS*, *NRAS*, *EGFR*, and *PTEN*). Among these 62 mutations, only 14 were detected in plasma samples before treatment, eight of which were in patients with acquired resistance (21% of 38 patients), with the remaining 6 mutations in patients with primary resistance (40% of 15 patients; Fig. 2D; Table 2).

Structure modeling and functional analysis of the *PIK3CA* mutations

Structural modeling revealed that all of the *PIK3CA* point mutations identified in ctDNA (p.K944N, p.F930S, p.V955G, p.V955I, and p.K966E) and in FFPE tumor tissue (p.V952A and p.L938*) affected the structural configuration of the PIK3CA protein and the kinase activity. p.F930 is located in the ATP-binding pocket, p. K944, p.V952, and p.V955 are in the activation-loop, and p.K966 is in the coil region close to the c-lobe, which is thought to stabilize the kinase conformation (Fig. 2E–H).

In vitro functional assays of the *PIK3CA* mutations

To confirm the role of *PIK3CA* mutations in cetuximab resistance, DiFi cells were transfected with *PIK3CA* mutations p. K944N, p.V955G, p.V955I, p.K966E p.F930S, and p.V952A, as well as the truncation mutation p.L938* were generated. We performed Western blot assays for pAKT (phosphorylated AKT) and pERK in DiFi cells transfected with these *PIK3CA* mutations. Compared with nontargeting control cells, *PIK3CA* mutations p. K944N, p.V955G, p.V955I, and p.K966E markedly increased the phosphorylation levels of AKT and MAPK3/MAPK1 (ERK1/ERK2), which were not affected by the addition of cetuximab alone or in combination with 5-FU. While the *PIK3CA* mutations p.F930S and p.V952A, as well as the truncation mutation p.L938*, had a less effect on AKT and MAPK3/MAPK1 phosphorylation, especially in the presence of cetuximab and/or 5-FU (Fig. 3I).

Cell viability analysis suggested that in the presence of cetuximab in combination with 10 μmol/L 5-FU, compared with mock transfected cells, DiFi cells overexpressing p.K944N, p.V955G, p.

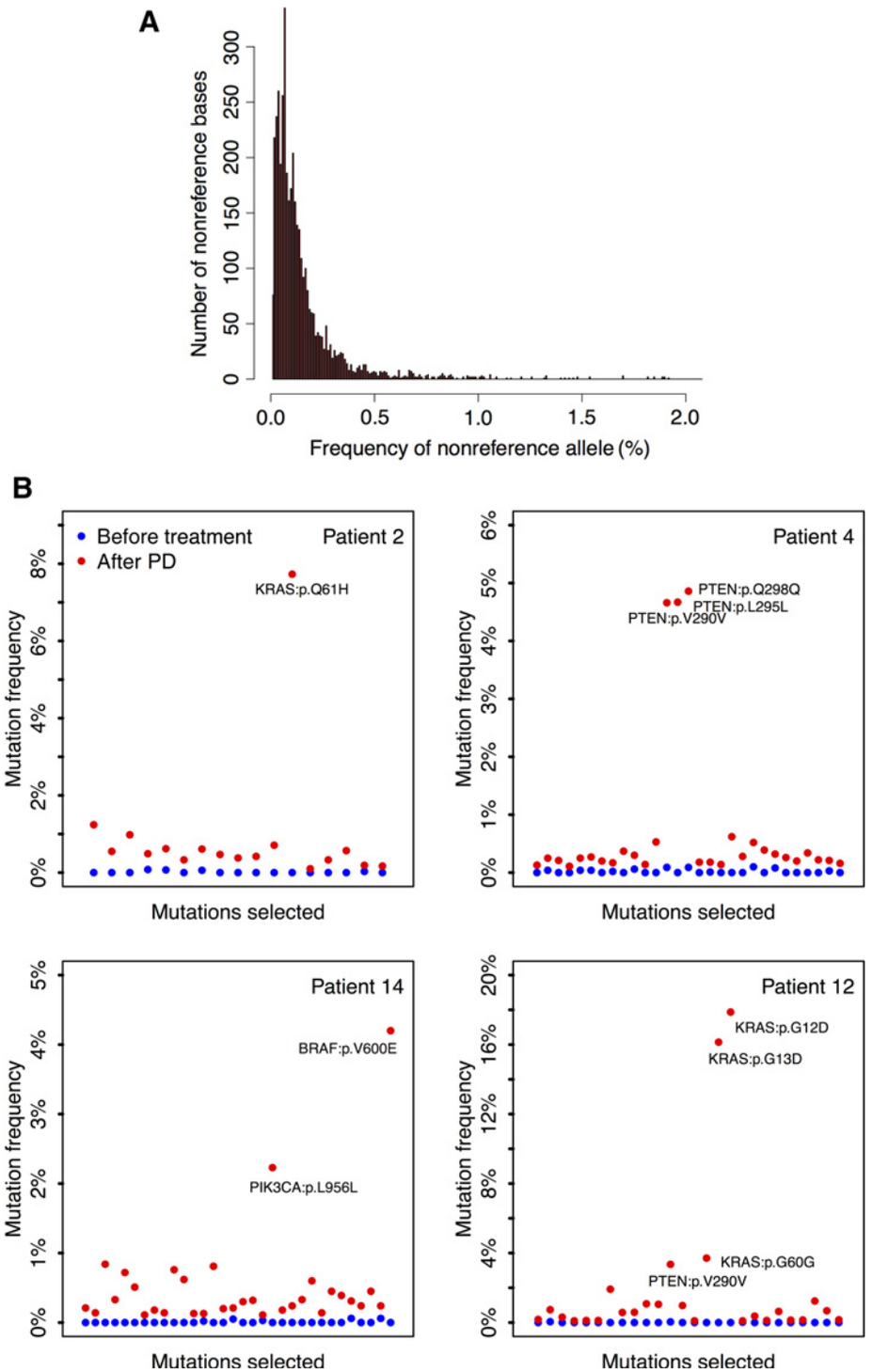

Figure 2.
Screening and functional analysis of acquired resistance related mutations. **A,** Distribution of the frequency of nonreference allele detected in circulating tumor DNA in a representative plasma sample. The majority of the single-nucleotide variants (SNVs) was present in very low allelic frequency (<0.5%). **B,** The frequencies of candidate mutations in four representative patients, before cetuximab treatment and after progressive disease (PD). Mutation frequencies were either significantly higher at disease progression or only present at disease progression. Quartile analysis was used to identify outliers. (*Continued on the following page.*)

V955I, p.K966E, p.E542K, p.E545K, and p.H1047R exhibited a high degree of resistance. Wild-type *PIK3CA*, as well as its p.F930S and p.V952A mutants, resulted in moderate resistance to cetuximab, and the truncation mutation p.L938* did not exhibit resistance. In the presence of 10 μg/mL cetuximab, growth rates in cells with novel *PIK3CA* mutations (p.K944N, p.F930S, p.V955G, p.V955I, and p.K966E) and with wild-type *PIK3CA* were 59.18 ± 14.72% versus 31.37%, respectively (Fig. 2J; Supplementary Fig. S2). These results demonstrate that these candidate mutations are likely to be involved in conferring resistance

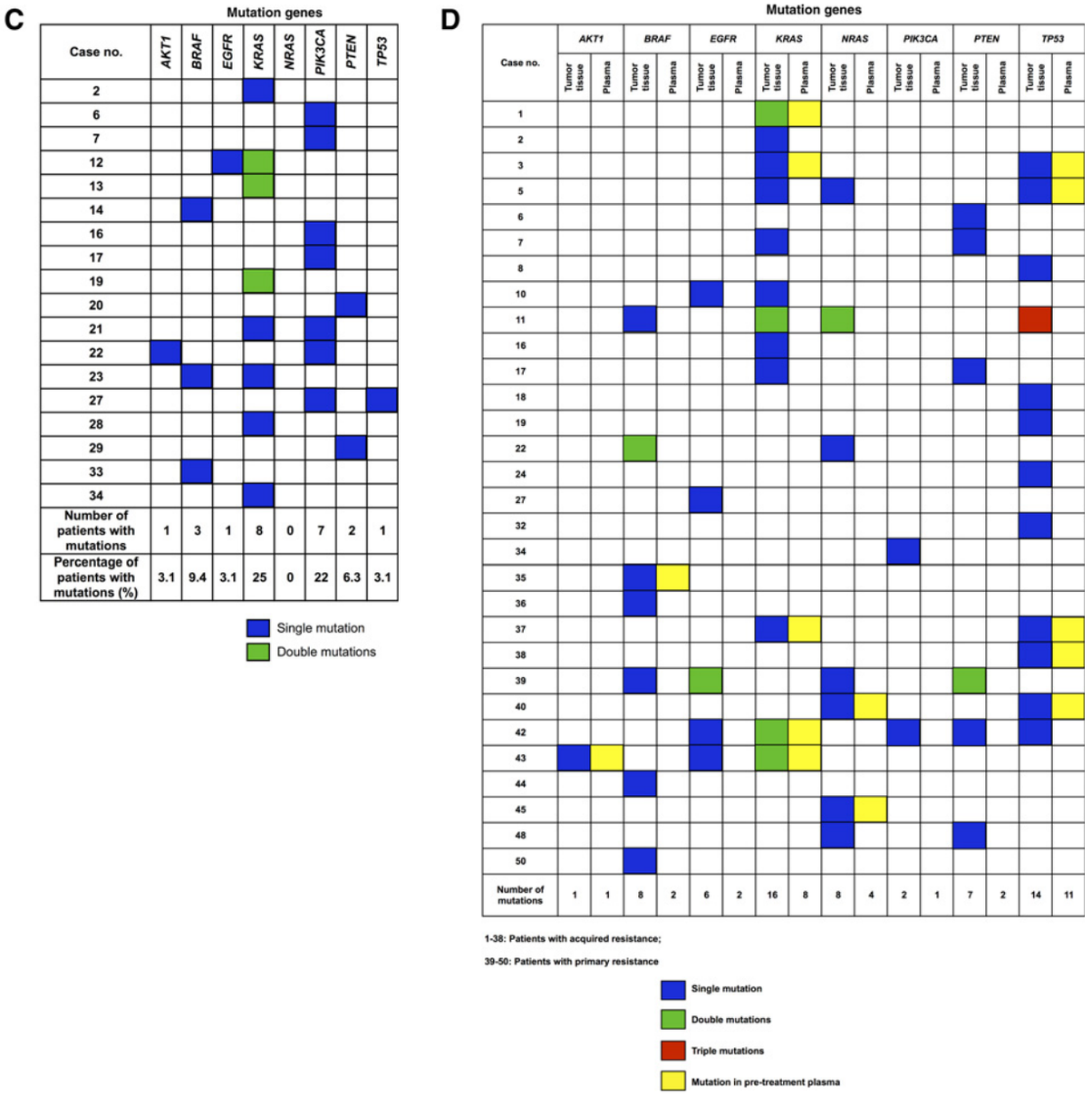

Figure 2.

(*Continued.*) **C,** Genetic mutations identified in the ctDNA of individual patients that were associated with acquired resistance to cetuximab. ctDNA, circulating tumor DNA. **D,** Genetic mutations detected in tumor tissue and in pretreatment plasma samples from individual patients. (*Continued on the following page.*)

because of their effects on the activation of the phosphorylation of AKT and MAPK3/MAPK1 (ERK1/ERK2).

Correlations among variant frequency, CEA and CA19-9 levels, and tumor response evaluation

Among the 20 patients with longitudinal plasma samples, 10 carried candidate mutations. We compared changes in the allelic fraction of the identified mutations in each patient with serum levels of corresponding tumor biomarkers and response ascertained using CT (as defined by RECIST; Fig. 3A–D and Supplementary Fig. S3). *PIK3CA* mutations were identified in four patients (Nos. 6, 7, 16, and 17), and *KRAS* mutations were identified in an additional four patients (Nos. 2, 12, 13, and 19). Only two of the 10 patients harbored mutations in other genes. Patient 14 harbored the *BRAF* p.V600E mutation, whereas patient 20 carried the *PTEN* p.Q245* mutation. These mutations exhibited an increasing allelic fraction during treatment (Table 1; Supplementary Table S3). Whereas, only five of the 10 patients had elevated CEA or CA19-9 levels that correlated well with the tumor response. The levels of candidate resistant mutations increased prior to clinical progression, as determined by CT scans. A median of 15.0 weeks of lead time (range, 0–35 weeks) was

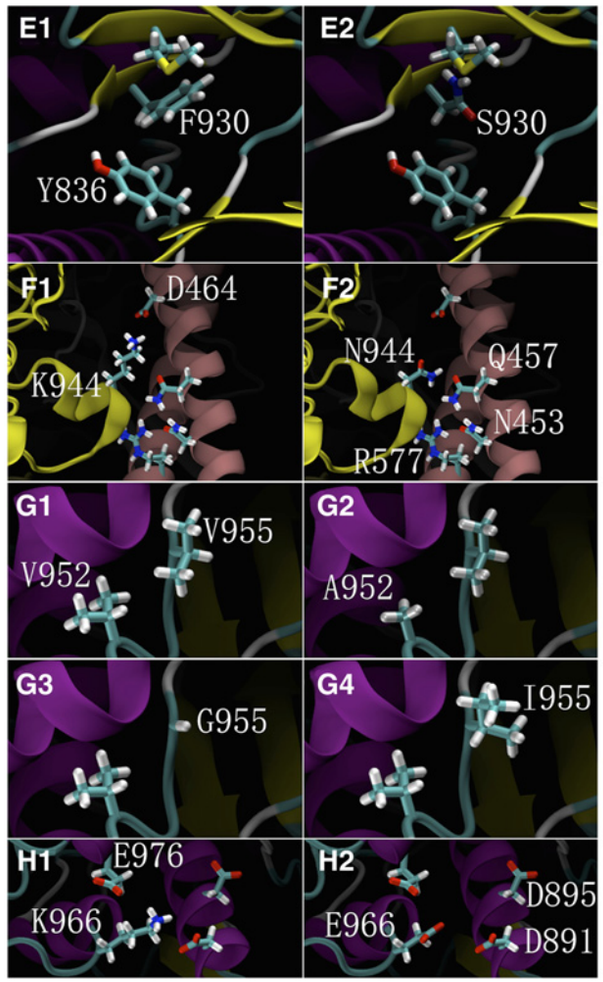

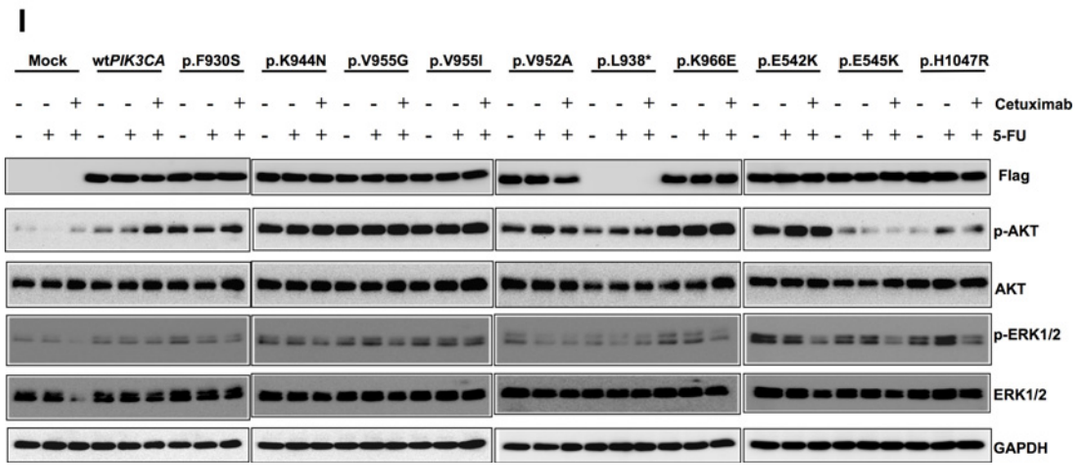

Figure 2.

(*Continued.*) **E1**, F930 can form a π interaction with Y836; **E2,** The F930S mutation abolishes the π interaction with Y836. **F1,** K944 can form an ionic bond with D464 in the α-regulatory subunit; **F2,** The K944N mutation abolishes the ionic bond interaction with D464, but it may form a hydrogen bond interaction with N453, Q457, and R577 in the α-regulatory subunit. Such interactions caused by these mutations would incur large conformational changes in the protein structure of PIK3CA. **G1,** V952 and V955 both feature hydrophobic side chains; **G2, G3,** The V952A and V955G mutations result in smaller and less hydrophobic side chains; **G4,** The V955I mutation results in a larger side chain with greater hydrophobicity. **H1,** K966 has a basic side chain, which can form ionic interactions with the acidic side chains of E976, D891, and D895. **H2,** K966E changes the basic side chain to acidic, resulting in repellent interactions with other acidic side chains. **I,** Activation of AKT and ERK1/2 by *PIK3CA* mutations. Western blots depicting the phosphorylation levels of AKT and ERK1/2 in DiFi cells overexpressing wild-type and mutant *PIK3CA* (p.F930S, p.K944N, p.V955G, p.V955I, p.K966E, p.L938*, p.V952A, p.E542K, p.E545K, and p.H1047R) cultured in serum-free media and treated with 100 nmol/L cetuximab and/or 10 μmol/L 5-FU. (*Continued on the following page.*)

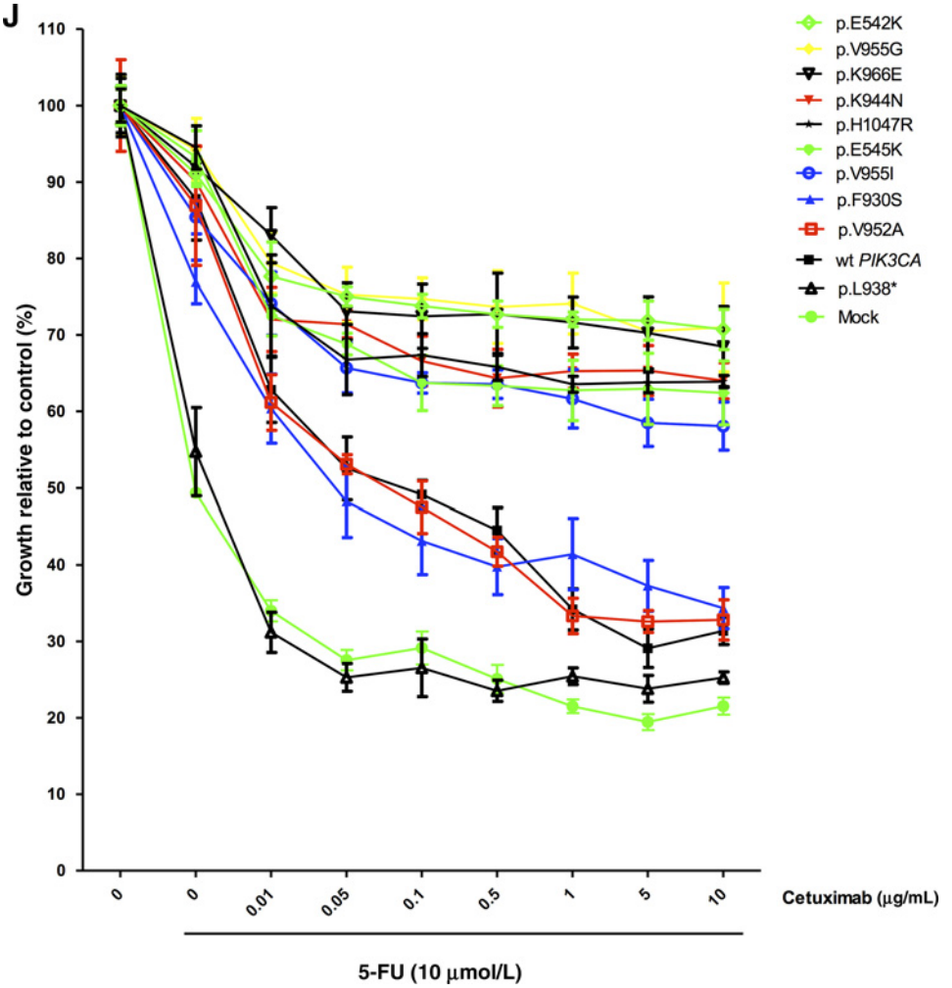

Figure 2.

(*Continued.*) **J,** Differential growth of DiFi cells transfected with wild-type *PIK3CA* or mutant *PIK3CA* in response to cetuximab and 5-FU, ordered by the relative sensitivity to cetuximab and 5-FU. The data are presented as the mean ± SD of six independent experiments. The assays were performed in serum-free media with increasing concentrations of cetuximab in combination with 5-FU at IC_{50}. wt *PIK3CA*: wild-type *PIK3CA*.

observed. In patients carried *PIK3CA* mutations, the average lead time was 10.8 weeks, whereas in patients with *KRAS* mutations, the average lead time was 21.8 weeks (Supplementary Table S1).

Additional mutation analysis in the validation cohort

An independent validation cohort of 32 patients (cases v1–v32) was prospectively enrolled between January 2014 and June 2016 to verify the acquired resistance mutations detected in the ctDNA of patients from the development cohort. Five patients (cases v1, v3, v9, v17, and v18) were placed in the primary resistance group, whereas the remaining 27 patients were classed as having acquired resistance (Table 3; Supplementary Table S4).

Thirty-seven mutations were identified in 14 of the 27 patients with acquired resistance, including one novel *PIK3CA* mutation (p.K944N) and the hotspot mutations p.V600E in *BRAF;* p.G12V in *KRAS;* p.G12V, p.G13V and p.Q61H in *NRAS;* p.H1047R and p.E545K in *PIK3CA*; and p.T790M in *EGFR* (Supplementary Table S5, Supplementary Fig. S4). Among these 14 patients, five patients carried multiple gene mutations, including two of them harbored both *KRAS* and *PIK3CA* hotspot mutations (case v5: p.H1047R in *PIK3CA* and p.M72V in *KRAS*; case v20: p.E545K, p.Q546K in *PIK3CA*, and p.G12V in *KRAS*). Other novel mutations in *PIK3CA* (p.F930S, p.V955G, p.V955I, and p.K966E) identified in the initial cohort were not detected in patients in this validation cohort. Although p.V600E in *BRAF* and p.G12V in *KRAS* were the only mutations verified in both cohorts due to the limited sample size and increased gene regions for sequencing in validation cohort, the identification of aforementioned hotspot mutations testified the reliability of the results in this validation cohort. No acquired resistance mutations were detected in the five patients with primary resistance in the validation cohort.

Clinical features and prognostic value of mutation profiles and the clinical implications

The relationship between tumor location and *RAS* or *PIK3CA* mutations were compared. We first analyzed *RAS* and *PIK3CA* mutations in tumor tissue before cetuximab treatment. In the 13 cases with right-sided colon, *RAS* mutation rate was 38.5% (5/13) and *PIK3CA* mutation rate was 7.7% (1/13); In the 38 cases with left-sided colon, *RAS* mutation rate was 31.6% (12/38) and *PIK3CA* mutation rate was 2.6% (1/38; Supplementary Table S6).

We also analyzed differences of acquired *RAS* or *PIK3CA* mutations in ctDNA between left and right colons. In 17 patients with right-sided colon, the *RAS* mutation rate was 23.5% (4/17) and the *PIK3CA* mutation rate was 11.8% (2/17); in 47 patients with left-sided colon, the *RAS* mutation rate was 19.1% (9/47), the *PIK3CA* mutation rate was 17% (8/47). No significant

Table 1. Mutations related to acquired cetuximab resistance

Case No.	Gene	Transcript Accession	Exon	Nucleotide (genomic)	Nucleotide (cDNA)	Amino acid (protein)	AF (%)	*P* Value
2	*KRAS*	NM_004985	3	Chr12:25380275 T>G	c.364T>G	Q61H	7.73	<0.0001
6	*PIK3CA*	NM_006218	19	Chr3:178948060 A>T	c.2832A>T	K944N	1.07	0.0005
7	*PIK3CA*	NM_006218	19	Chr3:178948091 G>A	c.2863G>A	V955I	1.21	<0.0001
12	*EGFR*	NM_005228	12	Chr7:55227909 G>A	c.1376G>A	G459E	1.24	0.032
12	*KRAS*	NM_004985	2	Chr12:25398284 C>T	c.35C>T	G12D	17.87	<0.0001
12	*KRAS*	NM_004985	2	Chr12:25398281 C>T	c.38C>T	G13D	16.14	<0.0001
13	*KRAS*	NM_004985	2	Chr12:25398284 C>T	c.35C>T	G12D	2.29	<0.0001
13	*KRAS*	NM_004985	2	Chr12:25398281 C>T	c.38C>T	G13D	2.31	<0.0001
14	*BRAF*	NM_004333	15	Chr7:140453136 A>T	c.1799T>A	V600E	4.2	<0.0001
16	*PIK3CA*	NM_006218	19	Chr3:178948060 A>T	c.2832A>T	K944N	1.52	0.0001
17	*PIK3CA*	NM_006218	19	Chr3:178948060 A>T	c.2832A>T	K944N	1.12	0.0081
19	*KRAS*	NM_004985	2	Chr12:25398284 C>T	c.35C>T	G12D	3.87	<0.0001
19	*KRAS*	NM_004985	2	Chr12:25398281 C>T	c.38C>T	G13D	2.92	<0.0001
20	*PTEN*	NM_000314	7	Chr10:89717708 C>T	c.733C>T	Q245[a]	1.15	<0.0001
21	*KRAS*	NM_004985	4	Chr12:25378686 C>A	c.312C>A	K104N	1.34	<0.0001
21	*PIK3CA*	NM_006218	19	Chr3:178948017 T>C	c.2789T>C	F930S	2.11	<0.0001
22	*PIK3CA*	NM_006218	19	Chr3:178948092 T>G	c.2864T>G	V955G	1.46	<0.0001
22	*AKT1*	NM_001014431	3	Chr14;105246536 A>C	c.64A>G	W22G	1.5	<0.0001
23	*BRAF*	NM_004333	15	Chr7:140453076 A>T	c.1859A>T	M620K	1.04	<0.0001
23	*KRAS*	NM_004985	2	Chr12:25398233 A>G	c.86A>G	V29A	1.65	<0.0001
27	*TP53*	NM_000546	5	Chr17:7578255 T>A	c.594T>A	E198D	1.57	<0.0001
27	*PIK3CA*	NM_006218	19	Chr3:178948124 A>G	c.2896A>G	K966E	1.72	<0.0001
28	*KRAS*	NM_004985	2	Chr12:25398304 T>G	c.15T>G	K5N	1.19	<0.0001
29	*PTEN*	NM_000314	5	Chr10:89692916 A>T	c.400A>T	M134L	1.15	<0.0001
33	*BRAF*	NM_004333	15	Chr7:140453181 T>C	c.1754T>C	H585R	1.13	<0.0001
34	*KRAS*	NM_004985	2	Chr12:25398284 C>A	c.35C>A	G12V	3.78	<0.0001

NOTE: *P* value: The differences of the identified mutant allelic fraction from the background non-reference allelic fractions were calculated using Student *t* test. Twenty-five of the 26 mutations exhibited a highly significant difference (*P* value < 0.01).
Abbreviation: AF, mutant allelic fraction of the last plasma sample.
[a]Stop-gain mutation.

differences were observed between left and right colons both in the *RAS* and *PIK3CA* mutation rate (Supplementary Table S7).

Next, we examined progression-free survival (PFS) from the clinical data of 65 patients with acquired resistance, to determine the relative prognostic value of mutation profiles and other clinical features. These patients consisted of 38 patients from the development cohort and 27 patients from the validation cohort.

Patients from the development cohort who had preexisting mutations in FFPE samples that were also present in ctDNA prior to treatment showed significantly shorter PFS compared with those without preexisting mutations in ctDNA (mPFS, 14 weeks vs. 38 weeks; HR, 2.69; 95% CI, 1.12–6.49; $P = 0.027$; Fig. 3E), respectively. We did not perform this analysis in the validation cohort due to the unavailability of FFPE samples.

A trend toward a shorter PFS was noted in patients with a residual primary tumor compared with those with no residual primary tumor (mPFS, 20 weeks vs. 41 weeks; HR, 1.71; 95% CI, 0.94–3.13; $P = 0.08$; Fig. 3F).

When comparing to patients with no mutation ($n = 27$) detected in ctDNA, patients with *PIK3CA* ($n = 7$) or *RAS* ($n = 10$) mutations showed a pronounced mPFS decrease, although without significant difference due to very small sample size (40 weeks vs. 38 weeks vs. 29 weeks; HR, 1.26; 95% CI, 0.79–2.01; $P = 0.34$; Fig. 3G). Taken together, these results suggest that preexisting mutations present in ctDNA, residual primary tumor and *RAS* mutations will be potentially negative factors for cetuximab treatment.

Discussion

In this study, our purpose was to investigate the potentially acquired resistance mutations in eight targeted genes after clinical benefit from cetuximab-based regimens. The prerequisite concerning the acquired resistance during the cetuximab therapy is the PFS $\geq$ 12 weeks. For this reason, we enrolled all mCRC patients with no previous anti-EGFR antibody treatment prior to study participation who would be treated with cetuximab-based regimen, no matter how many previous treatment lines patients experienced.

We sequenced targeted gene areas with deep coverage to identify emergent mutations in longitudinal plasma samples collected from patients with mCRC. Our quartile-based selection strategy helped us to identify mutations that started at extremely low allelic fractions but increased in frequency during treatment, independently of the identification of existing somatic mutations in tumor tissues or in known "hot-spots." We were therefore not only able to identify novel mutations associated with acquired resistance, but also to build an understanding of resistance in each patient, even those with diverse mutation profiles.

Previous studies have demonstrated that mutations in the EGFR signal transduction pathway, such as *RAS*, contribute resistance to cetuximab (30). However, whether the *PIK3CA* mutations at exon 9 and 20 that have been identified in tumor tissue are correlated with drug resistance remains controversial (5, 17, 31, 32). As in the previous study, Bettegowda and colleagues analyzed known "hot-spot" mutations in *NRAS*, *BRAF*, *EGFR*, and *PIK3CA* and concluded that *KRAS* mutation is the most important factor for acquiring resistance to anti-EGFR therapy. However, they did not identify any known *PIK3CA* mutations associated with the acquisition of resistance (13, 14).

For *PIK3CA*, we examined exons 8 and 19 instead of previously reported hotspot mutations in exon 9 and 20, because the hotspot

Table 2. Preexisting mutations in tumor tissue and presence in plasma before treatment

Case No.	Gene	Transcript Accession	Exon	Nucleotide (genomic)	Nucleotide (cDNA)	Amino acid (protein)	AF[a] in tumor tissue (%)	AF in plasma before treatment (%)	Source of tumor tissue[b]
1	*KRAS*	NM_004985	4	chr12:25378688 T>C	c.310T>C	p.K104E	7.41	—[c]	P
	KRAS	NM_004985	3	chr12:25380231 T>C	c.227T>C	p.E76G	5.13	1.09	
2	*KRAS*	NM_004985	2	chr12:25398245 T>G	c.74T>G	p.Q25P	5.41	—	P
3	*TP53*	NM_000546	7	chr17:7577121 G>A	c.817G>A	p.R273C	35.15	1.09	P
	KRAS	NM_004985	3	chr12:25380275 T>G	c.183T>G	p.Q61H	27.19	1.83	
5	*TP53*	NM_000546	5	chr17:7578263 G>A	c.586G>A	p.R196[d]	30.82	1.59	P
	KRAS	NM_004985	4	chr12:25378670 G>A	c.328G>A	p.P110S	8.11	—	
	NRAS	NM_002524	4	chr1:115252209 G>A	c.431G>A	p.T144I	6.45	—	
6	*PTEN*	NM_000314	8	chr10:89720654 A>C	c.805A>C	p.K269Q	6	—	P
7	*PTEN*	NM_000314	7	chr10:89717661 C>A	c.686C>A	p.S229[d]	6.67	—	P
	KRAS	NM_004985	2	chr12:25398285 C>T	c.34C>T	p.G12S	7.69	—	
8	*TP53*	NM_000546	5	chr17:7578266 T>A	c.583T>A	p.I195F	14.17	—	P
10	*KRAS*	NM_004985	4	chr12:25378609 G>A	c.389G>A	p.A130V	5.13	—	P
	EGFR	NM_005228	12	chr7:55227843 C>T	c.1310C>T	p.S437F	6.25	—	
11	*TP53*	NM_000546	6	chr17:7577566 T>C	c.715T>C	p.N239D	6.18	—	P
	TP53	NM_000546	6	chr17:577555 G>T	c.726G>T	p.C242[d]	5.85	—	
	TP53	NM_000546	7	chr17:7577085 C>T	c.853C>T	p.E285K	5.37	—	
	KRAS	NM_004985	2	chr12:25398314 G>A	c.5G>A	p.T2I	6.4	—	
	BRAF	NM_004333	15	chr7:140453124 C>T	c.1811C>T	p.W604[d]	5.1	—	
	NRAS	NM_002524	3	chr1:115256508 C>T	c.203C>T	p.R68K	6.86	—	
	KRAS	NM_004985	4	chr12:25378577 A>G	c.421A>G	p.F141L	5.75	—	
	NRAS	NM_002524	3	chr1:115256445 G>T	c.266G>T	p.S89[d]	6.98	—	
16	*KRAS*	NM_004985	2	chr12:25398285 C>T	c.34C>T	p.G12S	28.15	—	P
17	*KRAS*	NM_004985	2	chr12:25398284 C>A	c.35C>A	p.G12V	40.6	—	P
	PTEN	NM_000314	7	chr10:89717672 C>T	c.697C>T	p.R233[d]	13.73	—	
18	*TP53*	NM_000546	7	chr17:7577138 C>T	c.800C>T	p.R267Q	14.34	—	P
19	*TP53*	NM_000546	5	chr17:7578217 G>A	c.632G>A	p.T211I	23.08	—	P
22	*BRAF*	NM_004333	15	chr7:140453136 A>T	c.1799A>T	p.V600E	6.25	—	P
	BRAF	NM_004333	15	chr7:140453139 G>A	c.1796G>A	p.T599I	6.25	—	
	NRAS	NM_002524	2	chr1:115258685 C>T	c.97C>T	p.D33N	6.25	—	
24	*TP53*	NM_000546	5	chr17:7578263 G>A	c.586G>A	p.R196[d]	54.55	—	P
27	*EGFR*	NM_005228	10	chr7:55224507 A>G	c.1189A>G	p.T397A	5	—	P
32	*TP53*	NM_000546	5	chr17:7578262 C>T	c.587C>T	p.R196Q	8.16	—	M
34	*PIK3CA*	NM_006218	19	chr3:178948041 T>A	c.2813T>A	p.L938[d]	6.9	—	P
35	*BRAF*	NM_004333	15	chr7:140453136 A>T	c.1799A>T	p.V600E	44.35	3.77	M
36	*BRAF*	NM_004333	15	chr7:140453136 A>T	c.1799A>T	p.V600E	15	—	P
37	*TP53*	NM_000546	5	chr1:7578263 G>A	c.586G>A	p.R196[d]	25	17.54	M
	KRAS	NM_004985	2	chr12:25398284 C>T	c.35C>T	p.G12D	18.03	11.06	
38	*TP53*	NM_000546	7	chr17:7577121 G>A	c.817G>A	p.R273C	33.58	1.39	P
39	*PTEN*	NM_000314	8	chr10:89720654 A>T	c.805A>T	p.K269[d]	17.39	—	P
	PTEN	NM_000314	5	chr10:89693000 G>T	c.484G>T	p.D162Y	5.34	—	
	NRAS	NM_002524	2	chr1:115258744 C>T	c.38C>T	p.G13D	5.15	—	
	EGFR	NM_005228	10	chr7:55224522 A>G	c.1204A>G	p.T402A	6.22	—	
	EGFR	NM_005228	10	chr7:55224507 A>G	c.1189A>G	p.T397A	5.78	—	
	BRAF	NM_004333	15	chr7:140453182 G>A	c.1753G>A	p.H585Y	5.35	—	
40	*TP53*	NM_000546	7	chr17:7577120 C>T	c.818C>T	p.R273H	81.16	24.5	P
	NRAS	NM_002524	3	chr1:115256529 T>A	c.182T>A	p.Q61L	41.67	15.28	
42	*TP53*	NM_000546	7	chr17:7577138 C>T	c.800C>T	p.R267Q	7.64	—	M
	PTEN	NM_000314	5	chr10:89692890 A>G	c.374A>G	p.K125R	5.47	—	
	PIK3CA	NM_006218	19	chr3:178948083 T>C	c.2855T>C	p.V952A	7.44	—	
	KRAS	NM_004985	4	chr12:25378598 C>T	c.400C>T	p.A134T	5.49	—	
	KRAS	NM_004985	2	chr12:25398285 C>T	c.34C>T	p.G12S	27.27	11.93	
	EGFR	NM_005228	10	chr7:55224490 A G	c.1172A>G	p.E391G	6.25	—	
43	*KRAS*	NM_004985	3	chr12:25380276 T>C	c.182T>C	p.Q61R	6.47	—	M
	KRAS	NM_004985	3	chr12;25380275 T>A	c.183T>A	p.Q61H	5.04	17.57	
	EGFR	NM_005228	12	chr7:55227963 G>A	c.1430G>A	p.W477[d]	7.25	—	
	AKT1	NM_001014431	3	chr14:105246551 C>T	c.49C>T	p.E17K	17.24	25	
44	*BRAF*	NM_004333	15	chr7:140453136 A>T	c.1799A>T	p.V600E	24.42	—	P
45	*NRAS*	NM_002524	2	chr1:115258745 C>G	c.37C>G	p.G13R	34.82	37.97	P
48	*PTEN*	NM_000314	5	chr10:89692905 G>A	c.389G>A	p.R130Q	54.55	—	P
	NRAS	NM_002524	2	chr1:115258747 C>T	c.35C>T	p.G12D	30.43	—	
50	*BRAF*	NM_004333	15	chr7:140453136 A>T	c.1799A>T	p.V600E	18.28	—	P

[a]AF: mutant allelic fraction of the last plasma sample.
[b]Source of tumor tissue: P, primary tumor; M, metastatic lesion.
[c]–: Mutant allele under the detectable level.
[d]Stop-gain mutation.

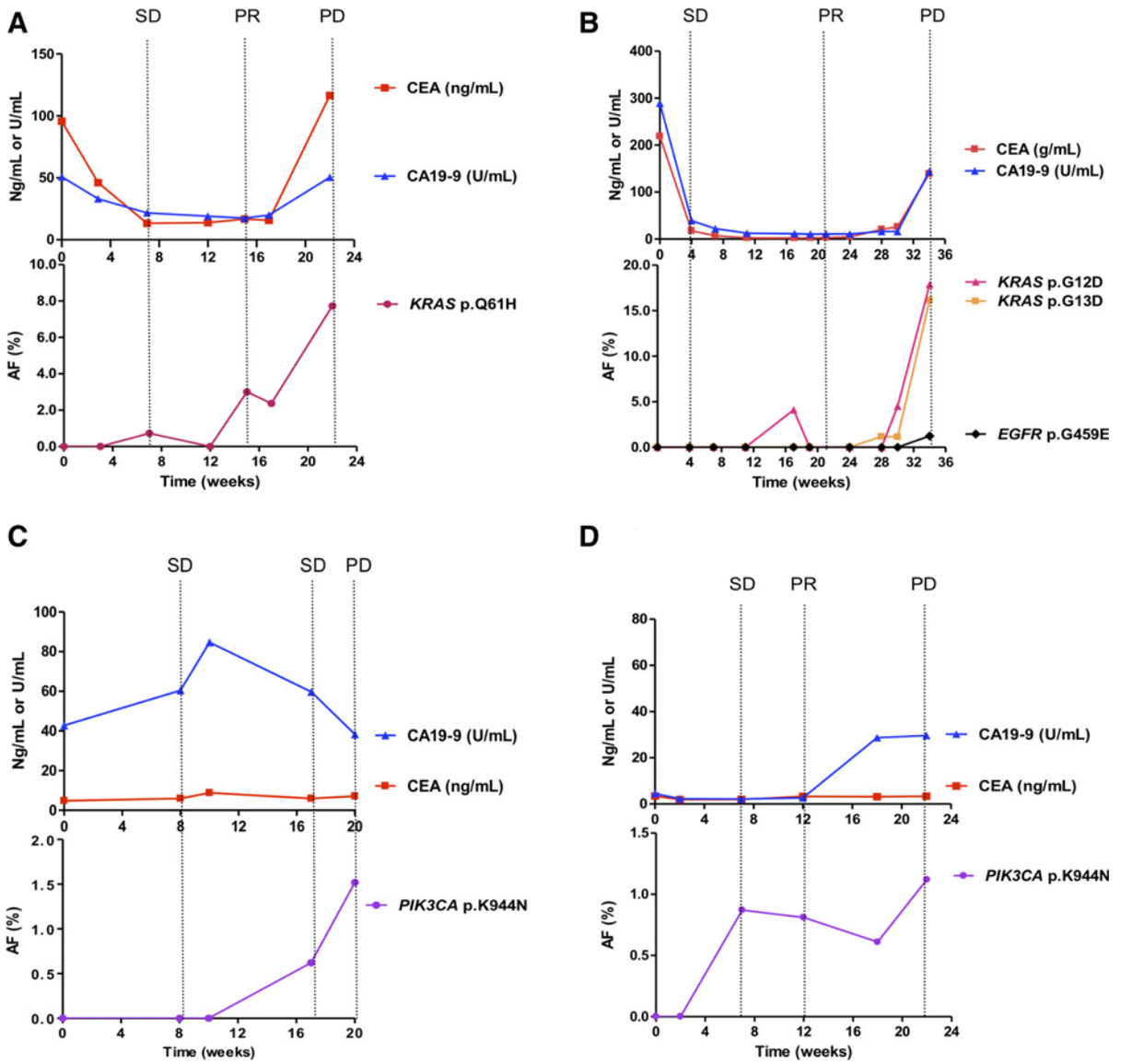

Figure 3.

Comparing circulating biomarkers with acquired resistant mutations used to monitor tumor dynamics and comparing different scenarios to predict progression-free survival. Each panel represents data from a different patient. **A,** case 2; **B,** case 12; **C,** case 16; **D,** case 17. Top panels, plasma levels of circulating biomarkers: CEA (ng per milliliter, red lines) and CA19-9 (U per milliliter, blue lines), over time (22 weeks). Lower panels show the allelic fractions (AFs) of mutations in the patient's circulating tumor DNA (ctDNA). Each color represents a specific mutation. Vertical dotted lines show the tumor response evaluation assessed according to RECIST criteria. PD, progressive disease; SD, stable disease; PR, partial response. (*Continued on the following page.*)

mutations in exons 9 and 20 were not identified in previous reports of acquired cetuximab resistance (13, 14). Bettegowda and colleagues had examined the acquired mutations of key genes in EGFR signaling pathway including *KRAS*, *NRAS*, *BRAF*, *EGFR*, and *PIK3CA* (exons 9 and 20) from ctDNA of 24 patients with mCRC during EGFR blockade. They observed 70 acquired mutations including *KRAS*, *NRAS*, *BRAF*, and *EGFR* (13). Siravegna and colleagues had monitored the acquired mutations of 226 genes, including *PIK3CA* (exon 20), in 16 patients with mCRC during anti-EGFR antibody therapy. They identified only *KRAS* and EGFR mutations. These two studies did not identify treatment-related mutations in exons 9 and 20 of the *PIK3CA* gene (14). Exon 8 encodes the region responsible for plasma membrane binding and exon 19 encodes part of the catalytic domain, including the ATP-binding pocket (33, 34). We reasoned that mutations in these *PIK3CA* sites might cause the constitutive activation of the kinase, similar to previously identified hotspot mutations (35, 36), although no any mutations in exons 8 and 19 had been reported in previous studies.

In this study, by analyzing different exons, we discovered five novel mutations in *PIK3CA* exon 19 in the development cohort

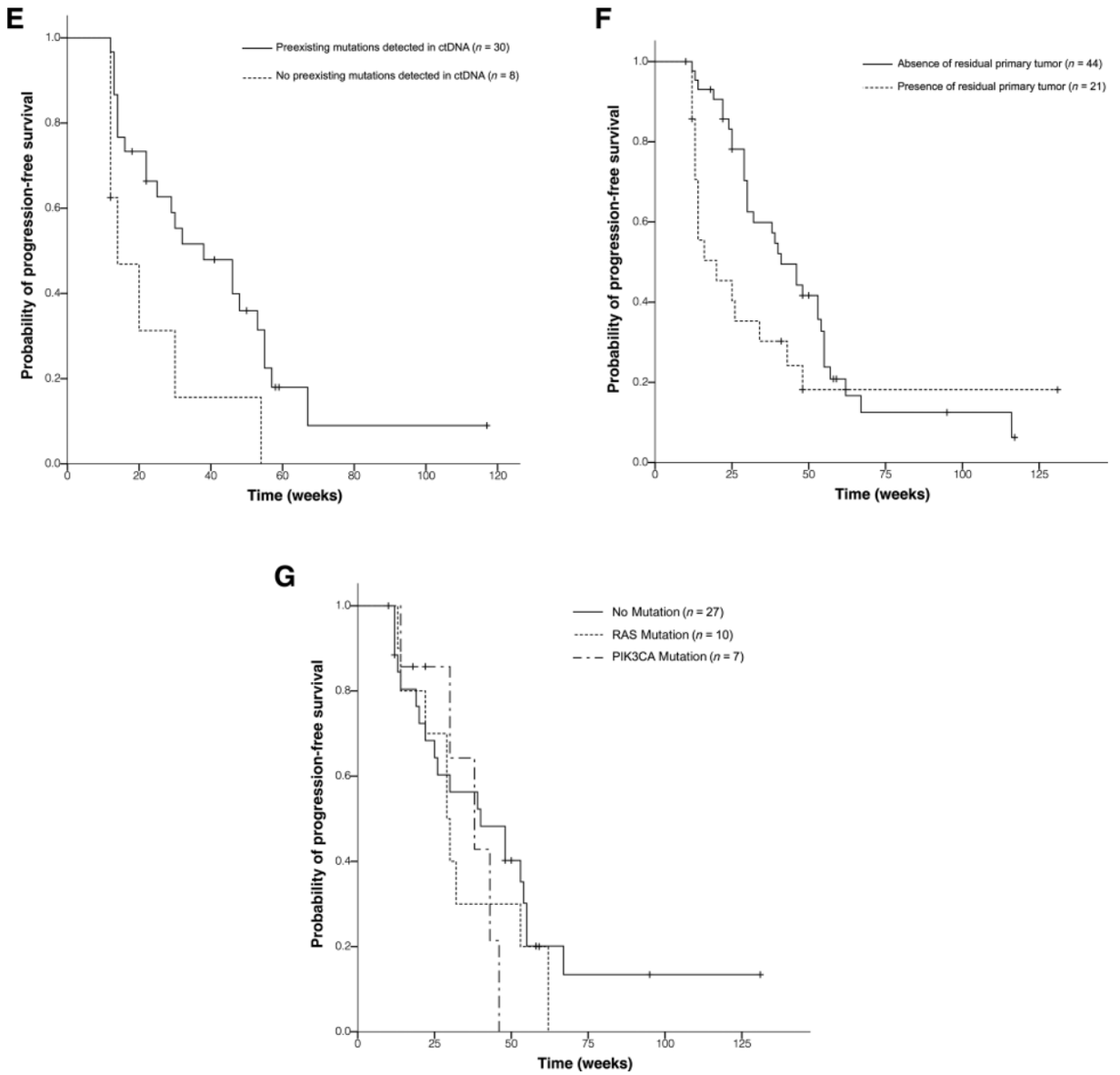

Figure 3.

(*Continued.*) **E** to **G,** each panel represents Kaplan–Meier survival functions for PFS, based on 65 patients with acquired cetuximab resistance. PFS, progression-free survival. ctDNA, circulating tumor DNA. **E,** Present formalin-fixed paraffin-embedded samples. Patients with mutations detected in ctDNA before treatment exhibit a significantly reduced PFS compared with those without any mutation in ctDNA (median PFS 14 weeks vs. 38 weeks; HR, 2.69; 95% CI, 1.12–6.49; $P = 0.027$). **F,** Patients with the presence of a residual primary tumor have a trend of shorter PFS compared with those without a residual primary tumor (mPFS, 20 weeks vs. 41 weeks; HR, 1.71; 95% CI, 0.94–3.13; $P = 0.08$). **G,** Comparing to patients with no mutation detected in ctDNA, patients with *PIK3CA* or *RAS* mutations showed a pronounced mPFS decrease, although without significant difference due to very small sample size (40 weeks vs. 38 weeks vs. 29 weeks; HR, 1.26; 95% CI, 0.79–2.01; $P = 0.34$).

and one novel mutation in exon 19, two "hot-spot" mutations in exons 9 and 20 in the validation cohort are closely associated with the development of resistance. Protein structure and functional assays revealed that all of these mutations would affect the structural configuration of PIK3CA, resulting in functional changes of protein. *In vitro* studies also demonstrated that novel *PIK3CA* mutations (p.K944N, p.V955G, p.V955I, and p.K966E) exhibited a high degree of resistance to cetuximab because of their effects on the activation of the phosphorylation of AKT and MAPK3/MAPK1 (ERK1/ERK2).

Analyses of molecular pathology and its interactions with environment are increasingly important in cancer research (37–42). As for the comparison of *RAS* or *PIK3CA* mutation rate of left- and right-sided colons, both *RAS* and *PIK3CA* mutation rates in tumor tissue were higher in the right-sided colon, which is consistent with findings in the literature reports (43–48),

Table 3. Clinical characteristics of acquired resistance patients in development cohort and validation cohort

Patient characteristics	Development cohort	Validation cohort	P^a
Age (year)			1
<65	32	23	
≥65	6	4	
Gender			1
Male	20	15	
Female	18	12	
ECOG			0.533
0	9	7	
1	24	19	
2	5	1	
Primary tumor location			0.775
Right side	9	8	
Left side	29	19	
Prior surgery			0.894
Radical resection	20	14	
Palliative resection	10	6	
None	8	7	
Residue of primary tumor			1
Yes	15	10	
No	23	17	
Line of prior therapy			0.002
<2 lines	17	23	
≥2 lines	21	4	
Regimen			<0.001
Cetuximab	19	1	
Cetuximab + chemotherapy	19	26	

[a]Fisher exact test.

although there were no significant differences due to small sample size. Whereas acquired *RAS* mutation is more frequent in the right colon, acquired *PIK3CA* mutation is more frequent in the left colon. Also, there were no significant differences due to small sample size.

We further compared the dynamics of acquired *RAS* and *PIK3CA* mutations in ctDNA and their influence on PFS. As compared with those with *KRAS* mutations, patients with *PIK3CA* mutations had a shorter lead time of presence of acquired mutations in ctDNA to clinical progression (21.8 vs.10.8 weeks). Patients harboring *PIK3CA* mutations exhibited increased median PFS, although the difference was not statistically significant due to the limited sample size. Because RAS is the upstream activator of the PI3K pathway (18, 49), we speculate that *PIK3CA* mutations in sites other than the RAS-binding domain are late-onset molecular events, relative to *RAS* mutations, that occur after exposure to cetuximab. These mutations might potentially exert a complementary effect in tumor progression and acquired resistance to cetuximab.

Another negative prognostic factor revealed in our study is the presence of residual primary tumor, which few studies in cetuximab treatment have mentioned. It is possible that when clones with wild-type genes are eliminated under the selective pressure of cetuximab, the remaining clones with preexisting and other emergent mutations in primary tumor would expand and display resistance over a relatively short time period, resulting in a shorter PFS. In the COIN clinical trial (50), which failed to demonstrate the survival benefit with the addition of cetuximab to chemotherapy, one underlying factor affect the survival benefit could be a substantial proportion of patients (>40%) with advanced CRC enrolled had unresected primary tumors. This independently supports our finding.

One limitation of this study is that the sample size in both cohorts was small. Larger sample size might help to discover more novel mutations, especially to distinguish the impact of clinical characters, such as tumor location (45, 48) and preexisting mutations on PFS between patients with and without acquired resistance mutations. Second, our present study focused only on the genomic variations analysis. Future investigation will be warranted to explore the potential mechanism beyond EGFR signaling pathway.

In summary, our data indicate that the *PIK3CA* mutations contribute to acquired cetuximab resistance in patients with mCRC. Compared with *RAS* mutations, which were reported to present before cetuximab treatment (8, 13, 14), *PIK3CA* mutations probably occur after exposure to cetuximab, and may potentially exert a complementary effect in acquired resistance to cetuximab.

Disclosure of Potential Conflicts of Interest

No potential conflicts of interest were disclosed.

Use of Standardized Official Symbols for Genes and Gene Products

We use HUGO (Human Genome Organisation)-approved symbols for genes and gene products, including AKT1, APC, BRAF, EGFR, GNAS, KRAS, MAPK1, MAPK3, NRAS, PIK3CA, PIK3R1, PTEN, and TP53, all of which are described at www.genenames.org. Gene names are italicized, and gene product names are nonitalicized.

Authors' Contributions

Conception and design: J.-M. Xu, Y.-L. Wang, M. Ni, Z.-L. Tan
Development of methodology: Y.-L. Wang, Y. Wang, M. Ni
Acquisition of data (provided animals, acquired and managed patients, provided facilities, etc.): Y. Wang, Y.-L. Wang, T. Liu, L. Lin, F.-J. Ge, J.-Y. Gu, R. Jia, Y.L. Chen, R.-R. Liu, C.-H. Zhao, Z.-L. Tan, Y. Jin
Analysis and interpretation of data (e.g., statistical analysis, biostatistics, computational analysis): J.-M. Xu, Y. Wang, Y.-L. Wang, Y. Wang, M. Ni, M.-S. Li, C. Gong, Z.-L. Tan, Y. Zhu, S. Ogino, Z.R. Qian
Writing, review, and/or revision of the manuscript: J.-M. Xu, Y. Wang, Y.-L. Wang, R. Jia, S. Ogino, Z.R. Qian
Administrative, technical, or material support (i.e., reporting or organizing data, constructing databases): Y. Wang, Y.-L. Wang, H.-F. Wang
Study supervision: J.-M. Xu, Y. Wang, Z.R. Qian

Acknowledgments

We thank all medical and ancillary staff at the Cancer Center and the patients for consenting to participate; Bo Zhang of the Department of Pathology for assistance with the preparation and assessment of formalin-fixed paraffin-embedded tumor samples; Xiang-Hua Zuo of the Clinical Laboratory for assistance with CEA and CA 19-9 analysis; Gong-Jie Li of the Department of Radiology for assistance with radiological response evaluation; and Su-Ping Lang and Chang-Hua Chen of GCP ClinPlus Co., Ltd., for their contribution to the statistical analysis; Peter Gorsuch, the scientific editor of Nature Research Editing Service, for their assistant in manuscript preparation.

Grant Support

This work was supported by the National Natural Science Foundation of China (to J. Xu, Y. Wang, F. Ge, and R. Jia; Project No. 81573458), the Translational Medicine Fund of Academy of Military Medical Sciences (to Y. Wang, J. Xu, Y. Wang, and R. Jia; Project No. 2013ZHYX006), the Chinese Society of Clinical Oncology Merck Serono Oncology Research Fund (to Y. Wang, J. Xu, Y. Wang, F. Ge, and R. Jia; Project No. Y-MX2014-052) the

U.S. National Institutes of Health (NIH) grant (to S. Ogino; R35 CA197735), and the Medical Oncology Translational Grant Program of Dana-Farber Cancer Institute(to Z.R. Qian).

The costs of publication of this article were defrayed in part by the payment of page charges. This article must therefore be hereby marked *advertisement* in accordance with 18 U.S.C. Section 1734 solely to indicate this fact.

Received October 31, 2016; revised December 6, 2016; accepted April 10, 2017; published OnlineFirst April 19, 2017.

References

1. Douillard JY, Oliner KS, Siena S, Tabernero J, Burkes R, Barugel M, et al. Panitumumab-FOLFOX4 treatment and RAS mutations in colorectal cancer. N Engl J Med 2013;369:1023–34.
2. Tejpar S, Stintzing S, Ciardiello F, Tabernero J, Van Cutsem E, Beier F, et al. Prognostic and predictive relevance of primary tumor location in patients with RAS wild-type metastatic colorectal cancer: retrospective analyses of the CRYSTAL and FIRE-3 trials. JAMA Oncol 2016 Oct 10. doi: 10.1001/jamaoncol.2016.3797. [Epub ahead of print].
3. Stintzing S, Modest DP, Rossius L, Lerch MM, von Weikersthal LF, Decker T, et al. FOLFIRI plus cetuximab versus FOLFIRI plus bevacizumab for metastatic colorectal cancer (FIRE-3): a post-hoc analysis of tumour dynamics in the final RAS wild-type subgroup of this randomised open-label phase 3 trial. Lancet Oncol 2016;17:1426–34.
4. Wang F, Bai L, Liu TS, Yu YY, He MM, Liu KY, et al. Right-sided colon cancer and left-sided colorectal cancers respond differently to cetuximab. Chin J Cancer 2015;34:384–93.
5. De Roock W, Claes B, Bernasconi D, De Schutter J, Biesmans B, Fountzilas G, et al. Effects of KRAS, BRAF, NRAS, and PIK3CA mutations on the efficacy of cetuximab plus chemotherapy in chemotherapy-refractory metastatic colorectal cancer: a retrospective consortium analysis. Lancet Oncol 2010;11:753–62.
6. Therkildsen C, Bergmann TK, Henrichsen-Schnack T, Ladelund S, Nilbert M. The predictive value of KRAS, NRAS, BRAF, PIK3CA and PTEN for anti-EGFR treatment in metastatic colorectal cancer: A systematic review and meta-analysis. Acta Oncol 2014;53:852–64.
7. Bronte G, Silvestris N, Castiglia M, Galvano A, Passiglia F, Sortino G, et al. New findings on primary and acquired resistance to anti-EGFR therapy in metastatic colorectal cancer: do all roads lead to RAS? Oncotarget 2015;6:24780–96.
8. Diaz LAJr, Williams RT, Wu J, Kinde I, Hecht JR, Berlin J, et al. The molecular evolution of acquired resistance to targeted EGFR blockade in colorectal cancers. Nature 2012;486:537–40.
9. Misale S, Yaeger R, Hobor S, Scala E, Janakiraman M, Liska D, et al. Emergence of KRAS mutations and acquired resistance to anti-EGFR therapy in colorectal cancer. Nature 2012;486:532–6.
10. Thierry AR, Mouliere F, El Messaoudi S, Mollevi C, Lopez-Crapez E, Rolet F, et al. Clinical validation of the detection of KRAS and BRAF mutations from circulating tumor DNA. Nat Med 2014;20:430–5.
11. Dawson SJ, Tsui DW, Murtaza M, Biggs H, Rueda OM, Chin SF, et al. Analysis of circulating tumor DNA to monitor metastatic breast cancer. N Engl J Med 2013;368:1199–209.
12. Murtaza M, Dawson SJ, Tsui DW, Gale D, Forshew T, Piskorz AM, et al. Non-invasive analysis of acquired resistance to cancer therapy by sequencing of plasma DNA. Nature 2013;497:108–12.
13. Bettegowda C, Sausen M, Leary RJ, Kinde I, Wang Y, Agrawal N, et al. Detection of circulating tumor DNA in early- and late-stage human malignancies. Sci Transl Med 2014;6:224ra24.
14. Siravegna G, Mussolin B, Buscarino M, Corti G, Cassingena A, Crisafulli G, et al. Clonal evolution and resistance to EGFR blockade in the blood of colorectal cancer patients. Nat Med 2015;21:795–801.
15. Van Cutsem E, Kohne CH, Lang I, Folprecht G, Nowacki MP, Cascinu S, et al. Cetuximab plus irinotecan, fluorouracil, and leucovorin as first-line treatment for metastatic colorectal cancer: updated analysis of overall survival according to tumor KRAS and BRAF mutation status. J Clin Oncol 2011;29:2011–9.
16. Eisenhauer EA, Therasse P, Bogaerts J, Schwartz LH, Sargent D, Ford R, et al. New response evaluation criteria in solid tumours: revised RECIST guideline (version 1.1). Eur J Cancer 2009;45:228–47.
17. Sood A, McClain D, Maitra R, Basu-Mallick A, Seetharam R, Kaubisch A, et al. PTEN gene expression and mutations in the PIK3CA gene as predictors of clinical benefit to anti-epidermal growth factor receptor antibody therapy in patients with KRAS wild-type metastatic colorectal cancer. Clin Colorectal Cancer 2012;11:143–50.
18. Martini M, De Santis MC, Braccini L, Gulluni F, Hirsch E. PI3K/AKT signaling pathway and cancer: an updated review. Ann Med 2014;46:372–83.
19. Dayem Ullah AZ, Lemoine NR, Chelala C. SNPnexus: a web server for functional annotation of novel and publicly known genetic variants (2012 update). Nucleic Acids Res 2012;40(Web Server issue):W65–70.
20. Ng PC, Henikoff S. SIFT: Predicting amino acid changes that affect protein function. Nucleic Acids Res 2003;31:3812–4.
21. Kumar P, Henikoff S, Ng PC. Predicting the effects of coding non-synonymous variants on protein function using the SIFT algorithm. Nat Protoc 2009;4:1073–81.
22. Reddy BV, Kaznessis YN. Use of secondary structural information and C alpha-C alpha distance restraints to model protein structures with MODELLER. J Biosci 2007;32:929–36.
23. Furet P, Guagnano V, Fairhurst RA, Imbach-Weese P, Bruce I, Knapp M, et al. Discovery of NVP-BYL719 a potent and selective phosphatidylinositol-3 kinase alpha inhibitor selected for clinical evaluation. Bioorg Med Chem Lett 2013;23:3741–8.
24. Brooks BR, Brooks CL3rd, Mackerell ADJr, Nilsson L, Petrella RJ, Roux B, et al. CHARMM: the biomolecular simulation program. J Comput Chem 2009;30:1545–614.
25. Liu T, Chen F, Tang N, Feng J, Zhao D, Wei K, et al. CD247 can bind SHC1, no matter if CD247 is phosphorylated. J Mol Recognit 2009;22:205–14.
26. Hsin J, Arkhipov A, Yin Y, Stone JE, Schulten K. Using VMD: an introductory tutorial. Curr Protoc Bioinformatics 2008;Chapter 5:Unit 5.7.
27. Giannakis M, Mu XJ, Shukla SA, Qian ZR, Cohen O, Nishihara R, et al. Genomic correlates of immune-cell infiltrates in colorectal carcinoma. Cell Rep 2016;17:1206.
28. Fecteau RE, Lutterbaugh J, Markowitz SD, Willis J, Guda K. GNAS mutations identify a set of right-sided, RAS mutant, villous colon cancers. PLoS One 2014;9:e87966.
29. Leto SM, Trusolino L. Primary and acquired resistance to EGFR-targeted therapies in colorectal cancer: impact on future treatment strategies. J Mol Med (Berl) 2014;92:709–22.
30. Bokemeyer C, Van Cutsem E, Rougier P, Ciardiello F, Heeger S, Schlichting M, et al. Addition of cetuximab to chemotherapy as first-line treatment for KRAS wild-type metastatic colorectal cancer: pooled analysis of the CRYSTAL and OPUS randomised clinical trials. Eur J Cancer 2012;48:1466–75.
31. Karapetis CS, Jonker D, Daneshmand M, Hanson JE, O'Callaghan CJ, Marginean C, et al. PIK3CA, BRAF, and PTEN status and benefit from cetuximab in the treatment of advanced colorectal cancer–results from NCIC CTG/AGITG CO.17. Clin Cancer Res 2014;20:744–53.
32. Sepulveda AR, Hamilton SR, Allegra CJ, Grody W, Cushman-Vokoun AM, Funkhouser WK, et al. Molecular biomarkers for the evaluation of colorectal cancer: guideline from the American Society for Clinical Pathology, College of American Pathologists, Association for Molecular Pathology, and American Society of Clinical Oncology. J Mol Diagn 2017;19:187–225.
33. Mandelker D, Gabelli SB, Schmidt-Kittler O, Zhu J, Cheong I, Huang CH, et al. A frequent kinase domain mutation that changes the interaction between PI3Kalpha and the membrane. Proc Natl Acad Sci U S A 2009;106:16996–7001.
34. Zhang D, Aravind L. Identification of novel families and classification of the C2 domain superfamily elucidate the origin and evolution of membrane targeting activities in eukaryotes. Gene 2010;469:18–30.
35. Zhao L, Vogt PK. Helical domain and kinase domain mutations in p110alpha of phosphatidylinositol 3-kinase induce gain of function by different mechanisms. Proc Natl Acad Sci U S A 2008;105:2652–7.

36. Samuels Y, Wang Z, Bardelli A, Silliman N, Ptak J, Szabo S, et al. High frequency of mutations of the PIK3CA gene in human cancers. Science 2004;304:554.
37. Ogino S, Chan AT, Fuchs CS, Giovannucci E. Molecular pathological epidemiology of colorectal neoplasia: an emerging transdisciplinary and interdisciplinary field. Gut 2011;60:397–411.
38. Colussi D, Brandi G, Bazzoli F, Ricciardiello L. Molecular pathways involved in colorectal cancer: implications for disease behavior and prevention. Int J Mol Sci 2013;14:16365–85.
39. Rescigno T, Micolucci L, Tecce MF, Capasso A. Bioactive nutrients and nutrigenomics in age-related diseases. Molecules 2017;22:105; doi:10.3390/molecules22010105.
40. Kocarnik JM, Shiovitz S, Phipps AI. Molecular phenotypes of colorectal cancer and potential clinical applications. Gastroenterol Rep 2015;3:269–76.
41. Manceau G, Marisa L, Boige V, Duval A, Gaub MP, Milano G, et al. PIK3CA mutations predict recurrence in localized microsatellite stable colon cancer. Cancer Med 2015;4:371–82.
42. Liao X, Lochhead P, Nishihara R, Morikawa T, Kuchiba A, Yamauchi M, et al. Aspirin use, tumor PIK3CA mutation, and colorectal-cancer survival. N Engl J Med 2012;367:1596–606.
43. Brule SY, Jonker DJ, Karapetis CS, O'Callaghan CJ, Moore MJ, Wong R, et al. Location of colon cancer (right-sided versus left-sided) as a prognostic factor and a predictor of benefit from cetuximab in NCIC CO.17. Eur J Cancer 2015;51:1405–14.
44. Inagaki D, Shiozawa M, Satoyoshi T, Atsumi Y, Murakawa M, Kazama K. Relationship between tumor location and oncogenes mutations (RAS, BRAF, and PIK3CA) in colorectal cancer. J Clin Oncol 2017; p suppl 4S; abstract 580.
45. Yamauchi M, Morikawa T, Kuchiba A, Imamura Y, Qian ZR, Nishihara R, et al. Assessment of colorectal cancer molecular features along bowel subsites challenges the conception of distinct dichotomy of proximal versus distal colorectum. Gut 2012;61:847–54.
46. Liao X, Morikawa T, Lochhead P, Imamura Y, Kuchiba A, Yamauchi M, et al. Prognostic role of PIK3CA mutation in colorectal cancer: cohort study and literature review. Clin Cancer Res 2012;18:2257–68.
47. Rosty C, Young JP, Walsh MD, Clendenning M, Walters RJ, Pearson S, et al. Colorectal carcinomas with KRAS mutation are associated with distinctive morphological and molecular features. Mod Pathol 2013;26:825–34.
48. Rosty C, Young JP, Walsh MD, Clendenning M, Sanderson K, Walters RJ, et al. PIK3CA activating mutation in colorectal carcinoma: associations with molecular features and survival. PLoS One 2013;8:e65479.
49. Castellano E, Sheridan C, Thin MZ, Nye E, Spencer-Dene B, Diefenbacher ME, et al. Requirement for interaction of PI3-kinase p110alpha with RAS in lung tumor maintenance. Cancer Cell 2013;24:617–30.
50. Maughan TS, Adams RA, Smith CG, Meade AM, Seymour MT, Wilson RH, et al. Addition of cetuximab to oxaliplatin-based first-line combination chemotherapy for treatment of advanced colorectal cancer: results of the randomised phase 3 MRC COIN trial. Lancet 2011;377:2103–14.